2008 IEEE International Conference on
Robotics and Automation
Pasadena, CA, USA, May 19-23, 2008

Elementary Mechanical Analysis of Obstacle Crossing for Wheeled Vehicles

Matthew D. Berkemeier, Eric Poulson, and Travis Groethe

***Abstract*— In this paper we model a wheeled UGV in an elementary manner to determine the effect of obstacle height on major design parameters, such as wheel size, wheelbase, and center of mass height. We consider both static and dynamic modeling approaches and find that consideration of dynamics allows for more freedom in parameter choice.**

I. Introduction

Specifications for an autonomous wheeled vehicle will often include a maximum obstacle size which must be traversed. The obstacle size then affects the design in a major way, as it determines wheel size and subsequently the frame size, motor size, etc. One of the UGVs (Unmanned Ground Vehicles) we are building has a requirement that it must traverse obstacles up to 10 cm in height. It was not immediately obvious what wheel size should be chosen to accomplish this requirement, nor was it clear what the wheelbase should be. In addition, the UGV is required to have an arm on top, and this will tend to make a high center of mass. We felt analysis was necessary to understand how all these factors would affect each other, and we were not aware of any previous work on this topic. Figure 1 shows an early concept and final photo of our robot.

Fig. 1. Early Concept and Final Prototype of the UGV Modeled in This Paper.

II. Background

Historically, the design of wheeled vehicles with obstacle crossing ability has been largely subjective and based on experience. In recent years, several tools have been developed to aid this process, but these are numerical solutions and involve many parameters. In [1] Apostolopoulos presents a framework for the synthesis and evaluation of wheeled vehicle configurations. Configuration equations capture the relationships between the form and performance of a wheeled vehicle. The analysis is quasi-static, and is suitable for detailed analysis using many parameters including soil and tire mechanics. Krebs et al. [2] present a quasi-static general 2D solution for multi-body vehicles on arbitrary terrain. Balasubramanian and Balch [3] present a method of optimizing the energy expenditure of an over-actuated 2D robot in obstacle crossing. Halme et al. [4] and Webb [5] present similar methods of obstacle crossing which combine wheel and vertical suspension actuation. Vertical load is reduced or eliminated when a wheel encounters an obstacle. The load is transferred to other wheels, so that the wheel can overcome a large obstacle without large friction forces. Lauria et al. [6] present the design of an 8 wheel vehicle with active suspension and tactile wheels, and a more detailed method of crossing a large step. Our work provides a method for back-of-the-envelope estimation of vehicle capabilities based on few parameters. This allows a vehicle designer to make rapid assessments of both quasi-static and dynamic step crossing ability of design concepts early in the design process.

Supported in part by TACOM contract W56HZV-04-C-0705.

Berkemeier and Poulson are with Autonomous Solutions, Inc., 990 North 8000 West, Petersboro, UT 84325, USA. Groethe is now with Micron Technology, Inc., 8000 South Federal Way, Boise, ID 83707, USA. Corresponding author email: mattb@autonomoussolutions.com.

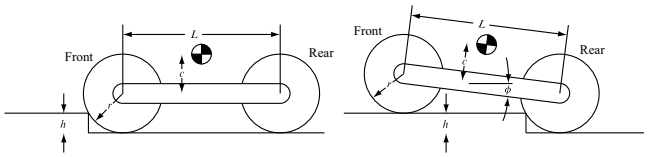

Fig. 2. Models for Vehicle Obstacle Crossing. Left: Both wheels Below the Obstacle. Right: One wheel Above the Obstacle.

III. Modeling

Notation for the dimensions of the model with both wheels below the obstacle are shown in Figure 2. r is the radius of both wheels, and L is the wheelbase. All of the mass is assumed to be concentrated at the vehicle midpoint, a distance c above the wheel centers. The height of the obstacle is h. When one wheel starts out above the obstacle, the situation is as shown in Figure 2. This adds the variable ϕ, which is the angle of the connecting bar with the horizontal.

A. Static Analysis

Figure 3 shows the forces which are assumed to act on the three parts of the model when both wheels begin below the obstacle. It would have been possible to do the analysis without breaking up the system into its three parts, and this would have been simpler. However, knowing the internal forces can be useful at times. For example, the torque at each wheel is internal to the system but would be useful for motor and gearing choices. Formulas for the torque and other

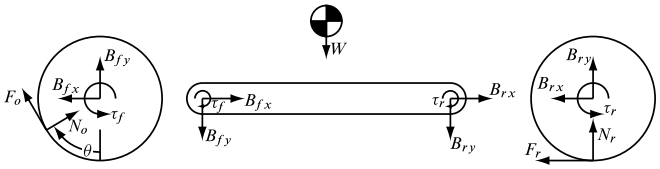

Fig. 3. Static Forces Acting on the Three Parts of the Model When Both Wheels Are Below the Obstacle.

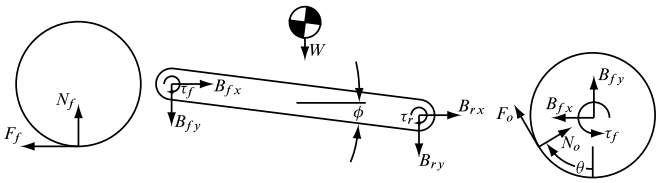

Fig. 4. Static Forces Acting on the Three Parts of the Model When One Wheel Is Above the Obstacle.

internal forces were not included in this paper but could be derived using the equations that are in the paper.

W is the total weight. F_o and N_o are the friction and normal forces from the obstacle (assumed to be tangential and normal to the wheel respectively) while F_r and N_r are the same forces at the rear wheel, which is on the ground. Simple Coulomb friction is assumed, with a friction coefficient of μ. The angle between the ground contact and the obstacle contact on the wheel is denoted by θ. Ground forces are not included on the front wheel because it was assumed the front wheel was about the leave the ground. τ_f and τ_r are the torques applied at the front and rear wheels respectively. B_{fx} and B_{fy} are the x and y components of the forces which constrain the front wheel to the bar, and a similar statement holds for B_{rx} and B_{ry}. The forces for one wheel starting up on the obstacle are shown in Figure 4. F_f and N_f are the front friction and normal forces.

From the geometry of the wheel and its contact point it is possible to derive the relationship between θ and h:

$$\cos\theta = 1 - \frac{h}{r},\ 0 < h < r \tag{1}$$

The following sections cover the two cases where both wheels are initially below the obstacle and where one wheel is initially above the obstacle.

1) Both Wheels Below: Referring to Figures 2 and 3, for the front wheel, the force and moment equations are

$$\begin{aligned} -F_o\cos\theta + N_o\sin\theta - B_{fx} &= 0 \\ F_o\sin\theta + N_o\cos\theta + B_{fy} &= 0 \\ \tau_f - F_o r &= 0 \end{aligned} \tag{2}$$

For the connecting bar we have

$$\begin{aligned} B_{fx} + B_{rx} &= 0 \\ -W - B_{fy} - B_{ry} &= 0 \\ B_{fy}\frac{L}{2} - B_{ry}\frac{L}{2} - \tau_f - \tau_r &= 0 \end{aligned} \tag{3}$$

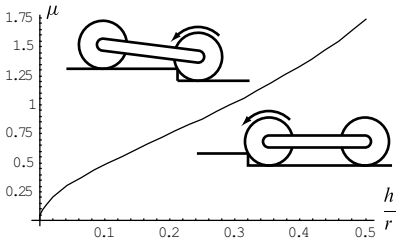

Fig. 5. Necessary Friction Coefficient When the Drive Wheel Is Against the Obstacle.

Finally, for the rear wheel,

$$\begin{aligned} -B_{rx} - F_r &= 0 \\ N_r + B_{ry} &= 0 \\ \tau_r - F_r r &= 0 \end{aligned} \tag{4}$$

$$\tau_r - F_r r = 0 \tag{5}$$

For the case of **front wheel drive**,

$$\tau_r = 0,\ F_o = \mu N_o$$

In this case the algebra is fairly simple. We see right away that $F_r = 0$ (equation 5). This implies that $B_{rx} = 0$ (equation 4), which implies that $B_{fx} = 0$ (equation 3). Finally, from equation 2 (with $F_o = \mu N_o$ and $B_{fx} = 0$) we arrive at the result

$$\boxed{\mu = \tan\theta} \tag{6}$$

This gives the necessary friction coefficient for a given step height since θ is directly related to h from equation 1. The result is shown in Figure 5.

For **rear wheel drive** we assume

$$\tau_f = 0,\ F_r = \mu N_r$$

The algebra is slightly more complicated this time. The final result is

$$\boxed{\mu = \frac{L\tan\theta}{L + 2r\tan\theta}} \tag{7}$$

In this case the friction needed depends not only on the contact angle θ but also on the wheelbase L. Figure 6 shows a plot of this result. As L/r gets large this result approaches the previous one in equation 6. For L/r small, there is a significant advantage to having the drive wheel push from behind, rather than being up against the obstacle (equation 6). The required coefficient in equation 7 is always smaller than in 6.

2) One Wheel Up: Referring to Figures 2 and 4, for the front wheel, the force and moment equations on the front wheel are

$$\begin{aligned} -F_f - B_{fx} &= 0 \\ B_{fy} + N_f &= 0 \\ \tau_f - rF_f &= 0 \end{aligned}$$

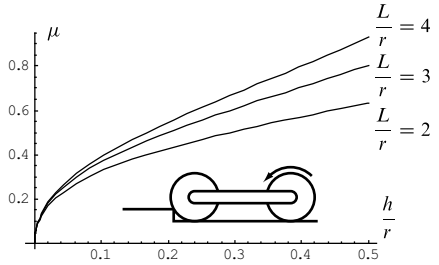

Fig. 6. Necessary Friction Coefficient When the Drive Wheel Is Down and the Passive Wheel Is Against the Obstacle.

For the connecting bar,

$$\begin{aligned} B_{fx} + B_{rx} &= 0 \\ -W - B_{fy} - B_{ry} &= 0 \\ B_{rx} L \sin\phi - B_{ry} L \cos\phi - & \\ W\left(\frac{L}{2}\cos\phi + c\sin\phi\right) - \tau_f - \tau_r &= 0 \end{aligned}$$

Finally, for the rear wheel,

$$\begin{aligned} -B_{rx} - F_o\cos\theta + N_o\sin\theta &= 0 \\ B_{ry} + N_o\cos\theta + F_o\sin\theta &= 0 \\ \tau_r - F_o r &= 0 \end{aligned}$$

For the case of **front wheel drive** we set

$$\tau_r = 0,\ F_f = \mu N_f$$

The end result is

$$\boxed{\mu = \frac{(L\cos\phi + 2c\sin\phi)\tan\theta}{L\cos\phi - 2(r\tan\theta + \sin\phi(c - L\tan\theta))}} \quad (8)$$

Also, from the geometry of Figure 2 we can determine that

$$\sin\phi = \frac{h}{L} \quad (9)$$

By combining equations 1, 8, and 9, we can produce the plots in Figure 7. Notice that this configuration of the vehicle model requires much more friction than the others. Also, equation 8 (out of 6, 7, 8) is the only equation that depends on the mass height, c. Smaller values of c appear to require smaller friction coefficients in Figure 7.

For **rear wheel drive**

$$\tau_f = 0,\ F_o = \mu N_o$$

The drive wheel is against the obstacle, and it turns out that the required friction is identical to case of front wheel drive with both wheels below the obstacle. The resulting equation is simply equation 6, which is plotted in Figure 5.

3) Discussion: For one of our vehicles we would like to use 45 cm diameter wheels, and we need to cross 10 cm obstacles. This means $h/r = 4/9$. Table I provides a few sample values from the formulas for this case. It seems clear that we should avoid the case where the drive wheel is on top of the obstacle, and we are trying to pull the passive wheel up. This seems to require the most friction (up to 162.894!).

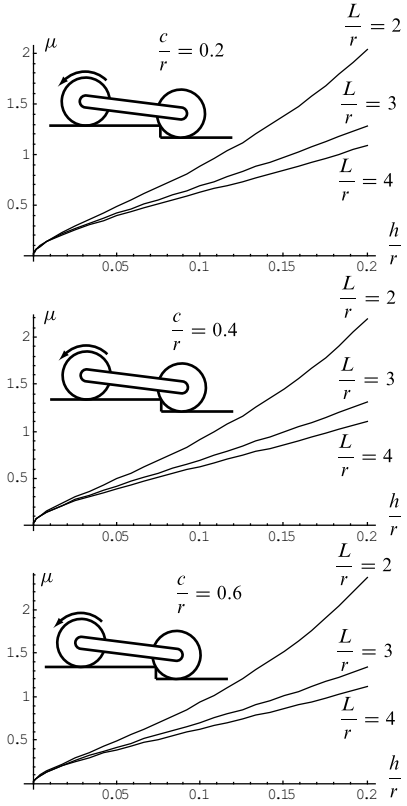

Fig. 7. Required Friction Coefficient When the Front Wheel Is Pulling the Rear Wheel Up.

Model Configuration	Coefficient Required	Parameter Values
Drive-wheel against obstacle	1.500	
Drive-wheel back, passive wheel against obstacle	0.599	$(L/r = 2)$
	0.856	$(L/r = 4)$
Drive-wheel up, passive wheel against obstacle	15.401	$(L/r = 2,\ c/r = 0.2)$
	2.653	$(L/r = 4,\ c/r = 0.2)$
	162.894	$(L/r = 2,\ c/r = 0.6)$
	2.822	$(L/r = 4,\ c/r = 0.6)$

TABLE I
REQUIRED FRICTION COEFFICIENTS FOR VEHICLE WITH 45 CM DIAMETER WHEELS AND A 10 CM OBSTACLE.

On the other hand, if we start out by pushing the passive wheel up, we need a much smaller friction coefficient (0.599 or 0.856). Once the passive wheel is up, the drive wheel will be against the obstacle, and a coefficient of 1.5 is required to finish crossing the obstacle. This is quite large but might be possible. More likely, a small amount of momentum can be used to reduce the required friction to a more reasonable amount. An analysis of the effect of momentum is the subject of the next section.

A short wheelbase helps when pushing the free wheel over the obstacle, but it hurts when we are trying to pull the free wheel up over the obstacle. If we plan to avoid the latter case, then we should try to make the wheelbase as small as possible.

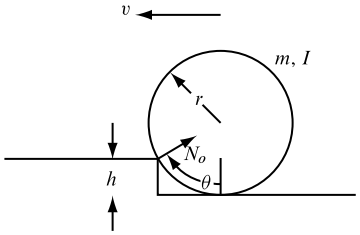

Fig. 8. Wheel Impact Model.

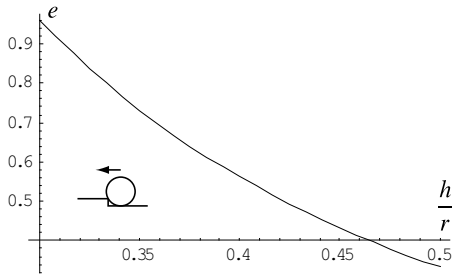

Fig. 9. Maximum Coefficient of Restitution for a Given Obstacle Height. The case of single wheel impact.

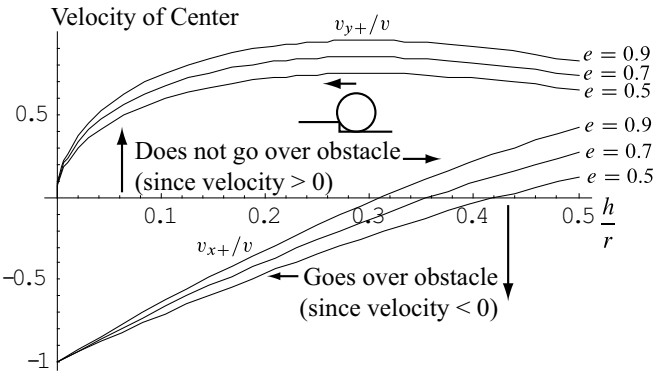

Fig. 10. Velocity of Wheel Center After Impact. The top curves are v_{y+}/v and the bottom curves are v_{x+}/v. For $v_{x+}/v < 0$ the wheel can go over the obstacle. For $v_{x+}/v > 0$ the wheel cannot.

B. Dynamic Analysis

1) Single Wheel: We found it helpful to start with just a simple wheel of mass m and inertia I about its center. Assume it initially has a speed v to the left in Figure 8, where the impulsive force N_o is also shown. After collision with the obstacle, the wheel center will have velocity components v_{x+} and v_{y+} as well as angular velocity ω_+.

The impulse-momentum equations [7] are

$$\begin{aligned} -mv + N_o \sin\theta &= mv_{x+} && (10)\\ N_o \cos\theta &= mv_{y+} && (11)\\ I\omega_- &= I\omega_+ \end{aligned}$$

Here, we have 3 equations and 4 unknowns (N_o, v_{x+}, v_{y+}, ω_+). The remaining equation involves the coefficient of restitution. The coefficient of restitution relates the relative speeds of 2 impacting objects just before impact to their relative speeds just after impact along the line of impact. The velocity of the contact point just before impact is

$$v\begin{bmatrix} \cos\theta - 1 \\ -\sin\theta \end{bmatrix}$$

Just after impact, the contact point will have velocity

$$\begin{bmatrix} v_{x+} \\ v_{y+} \end{bmatrix} + \omega_+ r \begin{bmatrix} \cos\theta \\ -\sin\theta \end{bmatrix}$$

The line of impact is given by $\pm[\sin\theta \ \cos\theta]^\mathsf{T}$. Projecting the velocities along the line of impact gives the final equation:

$$ev\sin\theta = v_{x+}\sin\theta + v_{y+}\cos\theta \qquad (12)$$

where $0 \le e \le 1$ is the coefficient of restitution. The solution to equations 10, 11, and 12 is

$$\begin{aligned} v_{x+} &= v((e+1)\sin^2\theta - 1)\\ v_{y+} &= v\frac{e+1}{2}\sin 2\theta \end{aligned}$$

We notice that $v_{y+} > 0$ for $0 < \theta < \pi/2$ (provided that $v > 0$). So, the wheel is always launched up into the air. On the other hand, for $v_{x+} < 0$ (headed over obstacle) we need

$$\boxed{\sin\theta < \frac{1}{\sqrt{e+1}}} \qquad (13)$$

This provides a bound on the coefficient of restitution to allow the traversal of a particular obstacle height since $\cos\theta = 1 - h/r$. Figure 9 shows the dependency of the coefficient of restitution on the obstacle height. This result shows that it is actually better to have soft, nonelastic wheels with high damping (giving low coefficients of restitution), to traverse larger obstacles. In particular, for our case where $h/r = 4/9$, we should have $e < 0.446$. Figure 10 shows the wheel center velocity just after impact.

2) Both Wheels Below: Next, we consider two wheels joined together by a rigid link as in Figure 2. The impact-momentum equations are given by

$$\begin{aligned} -m_w v_{x-} + N_0\sin\theta - B_{fx} &= m_w(v_{x+} + c\omega_+)\\ N_0\cos\theta + B_{fy} &= m_w\left(v_{y+} - \frac{L}{2}\omega_+\right)\\ I_w\omega_{f-} &= I_w\omega_{f+}\\ -mv_{x-} + B_{fx} + B_{rx} &= mv_{x+}\\ -B_{fy} - B_{ry} &= mv_{y+}\\ B_{fy}\frac{L}{2} - B_{ry}\frac{L}{2} + B_{fx}c + B_{rx}c &= I\omega_+\\ -m_w v_{x-} - B_{rx} &= m_w(v_{x+} + c\omega_+)\\ B_{ry} + N_r &= m_w\left(v_{y+} + \frac{L}{2}\omega_+\right)\\ I_w\omega_{r-} &= I_w\omega_{r+} \end{aligned}$$

In this case, N_0, B_{fx}, etc. are impulsive forces which act only at the instant of impact. We include $N_r > 0$ in the equations because, otherwise, the rear wheel will penetrate the ground. In addition, we add an equation to enforce the

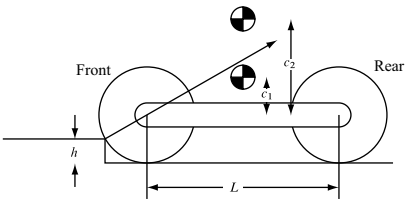

Fig. 11. Illustration of How COM Position Affects Obstacle Crossing.

non-penetration constraint for the rear wheel:

$$v_{x+} + \frac{L}{2}\omega_+ = 0$$

We simplify the equations slightly by setting $I_w = I = 0$, $m_w = 0$. We can solve for the velocity of the contact point after impact, $v_{x+} + c\omega_+$. However, the resulting equation is somewhat complicated and will not be presented here. It is more useful to instead consider the maximum possible coefficient of restitution for a given h/r which allows the vehicle to cross the obstacle. This is obtained by setting $v_{x+} + c\omega_+ = 0$ and solving for e. The result is

$$\boxed{e = \frac{4L\cot\theta(L\cos\theta - c\sin\theta)}{-4cL\cos\theta + (4c^2 + L^2)\sin\theta}} \tag{14}$$

However, there is a limit to the value of h/r. Whenever the center of mass lies above the line of impact, the vehicle will tend to flip over, rather than go over the obstacle. The condition for the center of mass being above the line of impact is given by

$$\frac{L}{2}\cot\theta > c \tag{15}$$

Consider Figure 11. For c_2 the impact will cause the vehicle to flip up with the rear wheel leaving the ground (In this case $N_r = 0$). For c_1 the rear wheel will stay on the ground ($N_r > 0$), and it is possible that the vehicle could cross the obstacle.

Figure 12 shows the result of equation 14. The curves end when inequality 15 is no longer satisfied.

3) One Wheel Up: We have also modeled the case where one wheel is on the step while the other impacts the step. The analysis is similar, and we will not include the derivation here. One small difference is that it seemed more logical to use the horizontal velocity of the center of mass just after impact in this case, rather than the horizontal velocity of the contact point in the both-wheels-below case. The final result for the maximum coefficient of restitution is

$$\boxed{e = \frac{(2\cos\phi(c + L\cot\theta) + L\sin\phi)^2}{(L\cos\phi + 2c\sin\phi)^2}}$$

where ϕ is the angle of the link with respect to the ground. (Note that it is derivable from other variables and parameters but simplifies the equation.) Plots generated from this equation are shown in Figure 13.

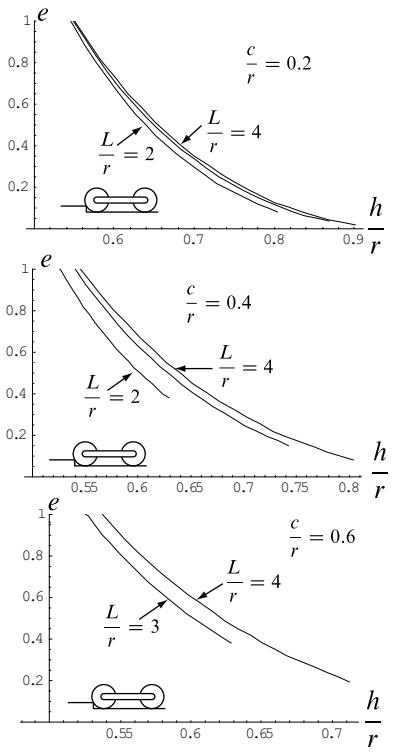

Fig. 12. Maximum Coefficient of Restitution When Both Wheels Start Below Obstacle.

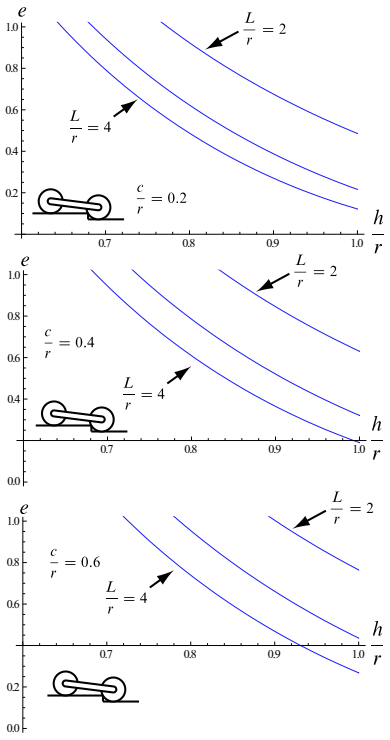

Fig. 13. Maximum Coefficient of Restitution When One Wheel Starts Above Obstacle.

Both Wheels Down	One Wheel Up	L/r	c/r
1.965	2.847	2	0.2
1.885	2.344	4	0.2
1.763	3.625	2	0.6
2.010	2.861	4	0.6

TABLE II

MAXIMUM COEFFICIENT OF RESTITUTION FOR VEHICLE WITH 45 CM DIAMETER WHEELS AND 10 CM OBSTACLE.

Fig. 14. Wheelchair Wheel Friction Measurement (top) and Wheelchair Against Step (bottom).

IV. EXPERIMENTS

Experiments were performed to determine the friction coefficient for a wheelchair wheel. An experiment is shown in Figure 14. Results ranging from 0.85 to 1.2 were obtained for the rubber wheel on a cinder block.

Experiments were also performed to test the analysis contained in the paper. Figure 14 shows one such experiment. Using 33.75 cm wheels and a cinder-block step, it was found that a 6.25 cm height ($h/r = 0.37$) could be traversed, while a 7.5 cm height ($h/r = 0.44$) could not. In the first case, the required friction coefficient from equation 6 is 1.23, which is similar to the 1.2 maximum value obtained experimentally. For the second case, the required coefficient is 1.50. This is significantly greater than the experimental value of 1.2, so there is apparent agreement between experiments and analysis. More experiments should be performed, however, since the scale readings shown in Figure 14 were not very repeatable.

We also performed experiments where our electric wheelchair was given a 30 cm running start before impacting a step. In this case, an 11.9 cm obstacle was traversed, while a 13.75 cm obstacle was not. Notably, the reason for the failure was due to the motor stalling, and this is not modeled in our analysis. In any case, equation 13 indicates that $e = 0.096$ is the maximum value for the 11.9 cm obstacle, while $e = 0.036$ is the maximum for the 13.75 cm obstacle. We experimentally determined e to be approximately 0.9, so the wheel should not traverse the obstacle in either case. It is possible that another effect was responsible for the wheel climbing over the obstacle. This might include wheel deformation and non-zero contact time between the wheel and step, which could have made motor torque non-negligible.

To help resolve this disparity between experiment and analysis, we performed another set of experiments. This time we used a single small rubber wheel with a 92 mm diameter. We determined its coefficient of restitution to be roughly 0.8. We then rolled it toward steps of different heights and observed whether the wheel bounced backward or forward after hitting the step. The wheel bounced backward on a step of height 23.1 mm, it bounced forward on a step of height 18.9 mm, and it seemed to bounce purely vertically on a step of height 20.8 mm (critical case). Equation 13 predicts the critical case would occur with a step height of 17 mm. So, the analysis and experimental results in this case still differ, but there is much better agreement than with the wheelchair. Again, the fact that the wheel can traverse a taller step than the analysis predicts could be due to the non-zero contact time and wheel deformation. The wheel deformation has the effect of effectively decreasing θ, which decreases the ratio h/r.

V. CONCLUSIONS

Static and dynamic analyses were performed to determine the effect of obstacle height requirements on major UGV parameters, such as wheel size, wheelbase, and center of mass height. We found that inclusion of dynamic effects led to a more relaxed set of constraints. Simple experiments provided rough verification of the analysis with exceptions noted and explained.

REFERENCES

[1] D. S. Apostolopoulos, "Analytical configuration of wheeled robotic locomotion," Ph.D. dissertation, Carnegie Mellon University, The Robotics Institute, Apr. 2001.

[2] A. Krebs, T. Thueer, S. Michaud, and R. Siegwart, "Performance optimization of all-terrain robots: A 2D quasi-static tool," in *2006 IEEE/RSJ International Conference on Intelligent Robots and Systems*, Oct. 2006, pp. 4266–4271.

[3] R. Balasubramanian and T. R. Balch, "Energy-optimal trajectories for overactuated robots," Carnegie Mellon University, The Robotics Institute, Tech. Rep., July 2002.

[4] A. Halme, I. Leppänen, M. Montonen, and S. Ylönen, "Robot motion by simultaneously wheel and leg propulsion," in *Proceedings of the 4th International Conference on Climbing and Walking Robots*, 2001, pp. 1013–1020.

[5] J. B. Webb, "Exploration of a hybrid locomotion robot," Master's thesis, Rochester Institute of Technology, Department of Mechanical Engineering, May 2007.

[6] M. Lauria, Y. Piguet, and R. Siegwart, "Octopus: an autonomous wheeled climbing robot," in *Proceedings of the Fifth International Conference on Climbing and Walking Robots*, 2002.

[7] R. C. Hibbeler, *Engineering Mechanics. Statics & Dynamics*, 8th ed. Prentice-Hall, Inc., 1997.